Randomized Manipulation Planning Considering the Local Optimization of Contact Mode Sequence

Masahito Yashima
National Defense Academy, Yokosuka 239-8686 JAPAN
yashima@nda.ac.jp

***Abstract*— This paper presents a randomized manipulation planner for a multi-fingered hand by switching contact modes. Manipulation planning for such a system should consider changing kinematics and dynamics of the system according to the contact modes. We derive the conditions that would be satisfied in manipulation planning, based on the properties of a manipulation system. The conditions give the restrictions of feasible contact modes and the number of contact points. Inspired by randomized motion planning techniques, we propose a new algorithm for manipulation planning in order to explore object configuration space rapidly and uniformly. Locally optimized contact modes are determined using a cost function. The basis for this approach is for the construction of exploring random trees. Simulation examples for 3-D manipulation by switching contact modes are presented to verify the planner's effectiveness.**

I. INTRODUCTION

Manipulating an object by a hand, we dextrously use different contact modes such as rolling and sliding contacts unconsciously. Utilizing different contact modes according to a manipulation task can raise manipulation skill with the hand. The primary motivation of our work is to manipulate the object by a multi-fingered robot hand utilizing different contact modes.

Work on manipulation by a multi-fingered robot hand has attracted attention. For example, there is work on manipulation with rolling and/or sliding contacts [2], [3], [7], [9], [12]. Most of the work has been devoted to the instantaneous kinematic and dynamic analysis of dextrous manipulation, assuming that there is no change of contact modes between the hand and object during a task. In contrast, since the kinematics and dynamics of the manipulation system changes according to the change of contact modes, we should consider manipulation planning taking into consideration the variable characteristics of the manipulation system in order to achieve our goal.

There is less work on manipulation planning [1], [10]. These work is restricted to a manipulation system with low degrees of freedom and quasi-static manipulation. Yashima and Yamaguchi [11] proposed an algorithm of dynamic manipulation planning, considering the characteristics of the manipulation system by changing contact modes. The dimension of search space is reduced by utilizing object nominal trajectory and randomly sampled switching times. However, the performance of the planner depends on the specified object nominal trajectory *a priori*.

The manipulation planning with changing contact modes is characterized by (i) huge search space, (ii) complicated constraint conditions for kinematics and dynamics and (iii) variable dynamics. Conventional methods based on the two-point boundary value problem, the problem of variation, dynamic programming, and so on cannot solve the above-mentioned manipulation planning. Recently, a new randomized motion planning algorithm based on the concepts of random trees has been shown to be valid for a uniform and rapid search of a high-dimensional state space. An algorithm known as rapidly exploring random trees (RRTs), was introduced by Lavalle and Kuffner [6]. The RRT algorithm consists of constructing a tree of feasible trajectories by extending branches toward randomly generated target points. Kindel et al. [5] developed another algorithm that, in order to build a new subgoal, a planner selects a control input at random and integrates the equations of motion under this control input from an existing subgoal. However, these algorithm mainly deals with the problem of determining collision-free trajectories that connect a given start to goal configuration for movable objects. Planning for manipulation by a multi-fingered hand is a complicated problem because of the nature of the contact such as rolling and sliding. To my knowledge, there is no study about manipulation planning from a randomized planning perspective.

In this paper, we first develop mathematical conditions that would be satisfied for manipulation planning, based on the properties of a manipulation system. These conditions give the restriction for feasible contact modes and the number of contact points. The dynamic problems for manipulation planning are not fully discussed here because the issues are already reported in my paper [11]. Inspired by randomized motion planning techniques, we propose a new algorithm for manipulation planning in order to explore object configuration space rapidly and uniformly. Locally optimized contact modes are determined using a cost function. The basis for this approach is for the construction of exploring random trees. Simulation examples for 3-D manipulation by switching contact modes are presented to verify the planner's effectiveness.

II. CONTACT MODES

A. Contact constraint

Fig.1 shows a manipulation system consisting of an object and a multi-fingered hand in space. We assume that each link of each finger has at most one contact point with the object, and each revolute joint has one degree of freedom. To describe the contact constraints between the object and the hand, we define a set of coordinate frames as follows: The reference frame, $\{U\}$, is fixed to the hand palm; the object frame, $\{O\}$, is fixed to the mass center of the object; the finger frame, $\{ij\}$, is fixed to the link of finger j with the ith contact point; The Gauss frame, $\{Oi\}$, of the object at the ith contact point are fixed relative to $\{O\}$. The Gauss frame, $\{Fi\}$, of the finger at the ith contact point is given similarly.

The relative linear velocities of $\{Oi\}$ relative to $\{Fi\}$ expressed in $\{Oi\}$ can be written as

$$\begin{bmatrix} v_{xi} \\ v_{yi} \\ v_{zi} \end{bmatrix} = \begin{bmatrix} \boldsymbol{G}_{xi}^T \\ \boldsymbol{G}_{yi}^T \\ \boldsymbol{G}_{zi}^T \end{bmatrix} \boldsymbol{V}_O - \begin{bmatrix} \boldsymbol{J}_{xij} \\ \boldsymbol{J}_{yij} \\ \boldsymbol{J}_{zij} \end{bmatrix} \dot{\boldsymbol{\theta}}_j \tag{1}$$

where $\boldsymbol{V}_O \in \Re^6$ is the linear and angular velocities of the object, and $\dot{\boldsymbol{\theta}}_j \in \Re^{n_{\theta j}}$ is the joint velocity of the jth finger. $n_{\theta j}$ indicates the number of joints of the jth finger. $\boldsymbol{G}_{xi}^T \in \Re^{1\times 6}$ is the matrix which maps $\boldsymbol{V}_O$ to the x-component of the contact velocity of the object expressed in $\{Oi\}$. $\boldsymbol{J}_{xij} \in \Re^{1\times n_{\theta j}}$ is the Jacobian matrix which maps $\dot{\boldsymbol{\theta}}_j$ to the x-component of the contact velocity of the finger expressed in $\{Oi\}$. Similarly, matrices $\boldsymbol{G}_{yi}^T$, $\boldsymbol{G}_{zi}^T$, $\boldsymbol{J}_{yij}$ and $\boldsymbol{J}_{zij}$ are defined.

On the other hand, the relative angular velocities of $\{Oi\}$ relative to $\{Fi\}$ expressed in $\{Oi\}$ can be written as

$$\begin{bmatrix} \omega_{xi} \\ \omega_{yi} \\ \omega_{zi} \end{bmatrix} = \begin{bmatrix} \widetilde{\boldsymbol{G}}_{xi}^T \\ \widetilde{\boldsymbol{G}}_{yi}^T \\ \widetilde{\boldsymbol{G}}_{zi}^T \end{bmatrix} \boldsymbol{V}_O - \begin{bmatrix} \widetilde{\boldsymbol{J}}_{xij} \\ \widetilde{\boldsymbol{J}}_{yij} \\ \widetilde{\boldsymbol{J}}_{zij} \end{bmatrix} \dot{\boldsymbol{\theta}}_j \tag{2}$$

where $\widetilde{\boldsymbol{G}}_{xi}^T \in \Re^{1\times 6}$ is the matrix which maps $\boldsymbol{V}_O$ to the x-component of the angular velocity of the object at the ith contact point expressed in $\{Oi\}$. $\widetilde{\boldsymbol{J}}_{xij} \in \Re^{1\times n_{\theta j}}$ is the Jacobian matrix maps $\dot{\boldsymbol{\theta}}_j$ to the x-component of the angular velocity of the finger at the ith contact point expressed in $\{Oi\}$. Similarly, matrices $\widetilde{\boldsymbol{G}}_{yi}^T$, $\widetilde{\boldsymbol{G}}_{zi}^T$, $\widetilde{\boldsymbol{J}}_{yij}$ and $\widetilde{\boldsymbol{J}}_{zij}$ are defined.

We will consider contact between two rigid bodies as shown in Fig.2. For a rolling contact, relative motions in x_i, y_i and z_i directions are constrained by corresponding contact forces, f_{Rxi}, f_{Ryi} and f_{Rzi}. Hence, the relative velocities, $v_{xi} = v_{yi} = v_{zi} = 0$, are required. On the other hand, a sliding contact requires $v_{zi} = 0$ by a normal contact force, f_{Szi}. Therefore the contact constraints on the rolling contact and sliding contacts can be written using (1) and (2) as

$$\begin{bmatrix} \boldsymbol{G}_{Rxi}^T \\ \boldsymbol{G}_{Ryi}^T \\ \boldsymbol{G}_{Rzi}^T \end{bmatrix} \boldsymbol{V}_O = \begin{bmatrix} \boldsymbol{J}_{Rxij} \\ \boldsymbol{J}_{Ryij} \\ \boldsymbol{J}_{Rzij} \end{bmatrix} \dot{\boldsymbol{\theta}}_j \quad \text{for rolling} \tag{3}$$

$$\boldsymbol{G}_{Szi}^T \boldsymbol{V}_O = \boldsymbol{J}_{Szij} \dot{\boldsymbol{\theta}}_j \quad \text{for sliding} \tag{4}$$

where subscripts R and S denote rolling and sliding contacts.

Summing (3) and (4) for all contacts yields

$$\boldsymbol{G}_A^T \boldsymbol{V}_O = \boldsymbol{J}_A \dot{\boldsymbol{\theta}} \tag{5}$$

where $\boldsymbol{G}_A \in \Re^{6\times(3n_R+n_S)}$ consists of $\boldsymbol{G}_{Rxi}$, $\boldsymbol{G}_{Ryi}$, $\boldsymbol{G}_{Rzi}$ and $\boldsymbol{G}_{Szi}$. Similarly, $\boldsymbol{J}_A \in \Re^{(3n_R+n_S)\times n_\theta}$ consists of $\boldsymbol{J}_{Rxij}$, $\boldsymbol{J}_{Ryij}$, $\boldsymbol{J}_{Rzij}$ and $\boldsymbol{J}_{Szij}$. There are n_C contacts, consisting of n_R rolling contacts and n_S sliding contacts. n_θ denotes the sum of joints.

According to Coulomb's law, the contact forces at rolling contacts lie within the boundary of its corresponding friction cone. The constraint on the ith contact forces can be written as nonlinear inequalities

$$\sqrt{f_{Rxi}^2 + f_{Ryi}^2} \le \mu_i f_{Rzi} \tag{6}$$

where μ_i is the coefficient of friction.

On the other hand, the contact forces at sliding contacts lie on the boundary of the corresponding friction cone and its tangential forces act on the object in the opposite direction to the motion of object relative to the hand at the contact point. Therefore the tangential contact forces, f_{Sxi} and f_{Syi}, in the ith contact frame are given by

$$f_{Sxi} = \widetilde{\mu}_{xi} f_{Szi}, \quad f_{Syi} = \widetilde{\mu}_{yi} f_{Szi} \tag{7}$$

where

$$\widetilde{\mu}_{\bullet i} = \frac{\mu_i v_{\bullet i}}{\sqrt{(v_{xi})^2 + (v_{yi})^2}}, \quad \bullet \in \{x, y\}$$

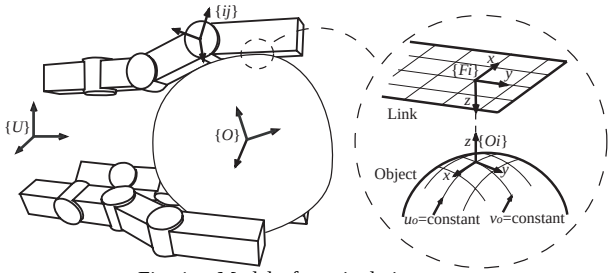

Fig. 1. Model of manipulation system

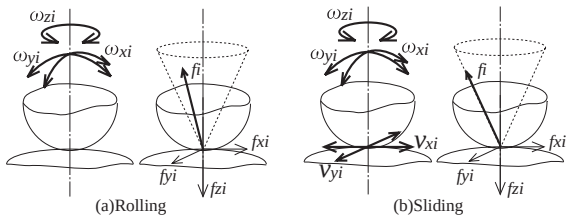

Fig. 2. Contact frictional forces and relative motions

When the object velocity, $\boldsymbol{V}_O$, is uniquely determined for a given joint velocity, $\dot{\boldsymbol{\theta}}$, the object motion can be restricted at each instant by the hand motion. A manipulation system satisfying this property is said to be kinematically determinate. Otherwise, there are infinite solutions for (5), and the object cannot be manipulated by the hand motion. From (5), the conditions for kinematically determinateness can be written as

$$3n_R + n_S \geq 6, \quad n_R + n_S = n_C, \quad \boldsymbol{G}_A \text{ is full rank} \tag{8}$$

Conversely, when we can find a joint velocity, $\dot{\boldsymbol{\theta}}$, which can accommodate an arbitrary object velocity, $\boldsymbol{V}_O$, a manipulation system is said to be kinematically manipulablity. From (5), the conditions for kinematically manipulable can be written as

$$3n_R + n_S \leq n_\theta, \quad \boldsymbol{J}_A \text{ is full rank} \tag{9}$$

These conditions for kinematicvally determinateness and manipulability in (8) and (9) are used to decide the feasibility of manipulation planning in the next section.

B. Dynamics

The dynamic equation of motion of rigid object can be written as

$$\boldsymbol{M}_O\dot{\boldsymbol{V}}_O = \boldsymbol{G}_{Rx}\boldsymbol{f}_{Rx}+\boldsymbol{G}_{Ry}\boldsymbol{f}_{Ry}+\boldsymbol{G}_{Rz}\boldsymbol{f}_{Rz}+\boldsymbol{G}_{\mu S}\boldsymbol{f}_{Sz}+\boldsymbol{g}_o \tag{10}$$

where $\boldsymbol{M}_o$ is the 6×6-mass matrix of the object, $\boldsymbol{g}_o$ is external wrench applied to the object, $\boldsymbol{G}_{\mu S} = \boldsymbol{G}_{Sx}\widetilde{\boldsymbol{\mu}}_x + \boldsymbol{G}_{Sy}\widetilde{\boldsymbol{\mu}}_y + \boldsymbol{G}_{Sz}$ and $\widetilde{\boldsymbol{\mu}}_\bullet = \mathrm{diag}[\cdots, \widetilde{\mu}_{\bullet i}, \cdots]$, $\bullet \in \{x, y\}$.

The motion equation of the hand can be written as

$$\boldsymbol{M}_H\ddot{\boldsymbol{\theta}} = \boldsymbol{\tau}-\boldsymbol{J}_{Rx}^T\boldsymbol{f}_{Rx}-\boldsymbol{J}_{Ry}^T\boldsymbol{f}_{Ry}-\boldsymbol{J}_{Rz}^T\boldsymbol{f}_{Rz}-\boldsymbol{J}_{\mu S}^T\boldsymbol{f}_{Sz}-\boldsymbol{g}_H \tag{11}$$

where $\boldsymbol{M}_H$ is the $n_\theta \times n_\theta$-inertia matrix of the hand, $\boldsymbol{g}_H$ is the vectors of joint torques caused by external wrenches and velocity product wrenches and $\boldsymbol{J}_{\mu S}^T = \boldsymbol{J}_{Sx}^T\widetilde{\boldsymbol{\mu}}_x + \boldsymbol{J}_{Sy}^T\widetilde{\boldsymbol{\mu}}_y + \boldsymbol{J}_{Sz}^T$.

III. RANDOMIZED MANIPULATION PLANNING

A. Global planning level

We discuss manipulation planning for three-dimensional manipulation by switching contact modes, based on the idea of random motion planning. In this paper, the aim of manipulation planning is to find optimal contact mode sequence as well as feasible trajectories of joint driving torques for the multi-fingered hand to manipulate the object from an initial configuration, $\boldsymbol{X}_{init}(\boldsymbol{R}_{Oinit},\ \boldsymbol{x}_{Oinit}) \in SE(3)$, to a specified final desired configuration, $\boldsymbol{X}_{goal}(\boldsymbol{R}_{Ogoal},\ \boldsymbol{x}_{Ogoal}) \in SE(3)$. We denote by $\boldsymbol{R}_O \in SO(3)$ and $\boldsymbol{x}_O \in \Re^3$ the orientation and the position of $\{O\}$ relative to $\{U\}$, respectively. We should note that both discrete state such as contact mode sequence, and time continuous state such as trajectories should be considered in this manipulation planning.

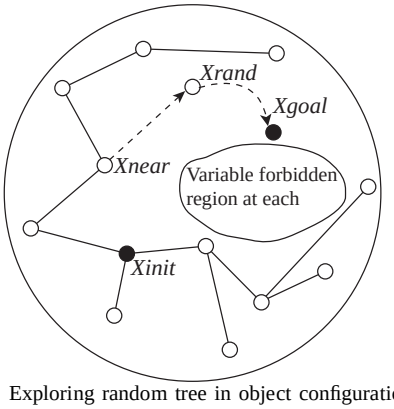

Fig. 3. Exploring random tree in object configuration space

The proposed algorithm of manipulation planning has a two-level planning scheme consisting of a global planning level and a local planning level. The global planner explores the object configuration space and constructs random trees extending to $\boldsymbol{X}_{goal}$. On the other hand, the local planner checks if feasible trajectories (trees) exist that connect subgoals (nodes). In this section, we present the algorithm of a global planner.

In the global planning level, it is necessary to explore the object configuration space rapidly and uniformly. Based on the ideas of random motion planning using the concepts of random trees, introduced by LaValle et.al.[6], we propose a novel algorithm for manipulation planning which explores a configuration space. Fig.3 illustrates exploring random trees in the object configuration space. The planner picks the candidate for subgoal, $\boldsymbol{X}_{rand} \in SE(3)$, at random in the object configuration space, then selects the nearest subgoal, $\boldsymbol{X}_{near}$, from $\boldsymbol{X}_{rand}$ from the existing random trees. Using a local planner to connect pairs of subgoals, $\boldsymbol{X}_{near}$ and $\boldsymbol{X}_{rand}$, the random trees are expanded in the configuration space. If the connection is not feasible, a new candidate, $\boldsymbol{X}_{rand}$, is re-selected at random. If the connection is feasible, the local planner tries again to connect $\boldsymbol{X}_{rand}$ to $\boldsymbol{X}_{goal}$. Also when the connection is feasible, the search is terminated. Otherwise, this process is performed iteratively until the random trees extend to $\boldsymbol{X}_{goal}$. Note that the forbidden region in Fig.3 is treated differently from an obstacle within a path planning problem since the forbidden regions vary at each instant based on the states of the manipulation system. Additionally, they are not already-known in the configuration space before executing the local planning.

The EXTEND_RANDOM_TREE function in Fig.4 shows the algorithm of the global planner. First, the REACHABLE function checks whether the local planner can connect $\boldsymbol{X}_{init}$ to $\boldsymbol{X}_{goal}$ directly. Unless there is such a trajectory connecting $\boldsymbol{X}_{init}$ to $\boldsymbol{X}_{goal}$, expanding random trees from $\boldsymbol{X}_{init}$ is executed iteratively. At each step, the RANDOM_CONFIG function selects a candidate for the object subgoal, $\boldsymbol{X}_{rand}$, at random in the object

EXTEND_RANDOM_TREE

1 if (REACHABLE($\boldsymbol{X}_{init}$, $\boldsymbol{X}_{goal}$)=TRUE) then STOP;
2 $\boldsymbol{X}_{rand} \longleftarrow$ RANDOM_CONFIG;
3 $\boldsymbol{X}_{near} \longleftarrow$ NEAREST_NEIGHBOR($\boldsymbol{X}_{rand}$);
4 if (REACHABLE($\boldsymbol{X}_{near}$, $\boldsymbol{X}_{rand}$)=TRUE) then
5 ADD_NEW_SUBGOAL($\boldsymbol{X}_{rand}$);
6 if (REACHABLE($\boldsymbol{X}_{rand}$, $\boldsymbol{X}_{goal}$)=TRUE) then STOP;
7 else goto the 2nd step;
8 else goto the 2nd step;

Fig. 4. Algorithm of EXTEND_RANDOM_TREE

configuration space. In order for subgoals to be distributed uniformly over the configuration space, the restriction of the range of exploration in the configuration space is imposed. We explore an object position, $\boldsymbol{x}_O$, within a sphere whose center is a middle point between $\boldsymbol{x}_{Oinit}$ and $\boldsymbol{x}_{Ogoal}$, and whose radius is $w_r\|\boldsymbol{x}_{Oinit} - \boldsymbol{x}_{Ogoal}\|$. The range of exploration for the position is determined by the value of the parameter $w_r \geq 1.0$. The object orientation relative to the initial orientation, $\boldsymbol{R}_{Oinit}$, can be represented by a rotation about an equivalent axis, $\widehat{\boldsymbol{k}} = [k_x \quad k_y \quad k_z]^T \in \Re^3$, by an equivalent angle, $\phi \in \Re^1$. The parameter ϕ is selected at random within $-\pi \leq \phi \leq \pi$. In order to assign the parameters $k_x,\ k_y$ and k_z at random, a point on the surface of a unit hemisphere expressed by $k_x^2 + k_y^2 + k_z^2 = 1$ is uniformly sampled.

The NEAREST_NEIGHBOR function chooses the nearest subgoal, $\boldsymbol{X}_{near}$, from $\boldsymbol{X}_{rand}$ according to a weighted Euclidean distance for position and orientation. A distance between subgoals $\boldsymbol{X}_A(\boldsymbol{R}_A, \boldsymbol{p}_A)$ and $\boldsymbol{X}_B(\boldsymbol{R}_B, \boldsymbol{p}_B) \in SE(3)$ is given by the form as:

$$\rho(\boldsymbol{X}_A,\ \boldsymbol{X}_B) = w_p\|\boldsymbol{p}_B - \boldsymbol{p}_A\| + w_\phi \cos^{-1}\left(\frac{\mathrm{Trace}(\boldsymbol{R}_A^T\boldsymbol{R}_B) - 1}{2}\right) \quad (12)$$

w_p and w_ϕ are weights for position and orientation respectively. ϕ_E is an equivalent rotation angle from $\boldsymbol{R}_A$ to $\boldsymbol{R}_B$. Then, the function REACHABLE($\boldsymbol{X}_{near}, \boldsymbol{X}_{rand}$) checks whether random trees can be expanded from $\boldsymbol{X}_{near}$ to $\boldsymbol{X}_{rand}$. If the random tree cannot reach from $\boldsymbol{X}_{near}$ to $\boldsymbol{X}_{rand}$, then we go back to the second step. Otherwise, the ADD_NEW_SUBGOAL function adds $\boldsymbol{X}_{rand}$ to the random trees as a new subgoal. In addition, REACHABLE($\boldsymbol{X}_{rand}, \boldsymbol{X}_{goal}$) checks whether random trees can be expanded from $\boldsymbol{X}_{rand}$ to $\boldsymbol{X}_{goal}$. If so, the exploration is terminated. Otherwise, we go back to the second step. The EXTEND_RANDOM_TREE is terminated when the iteration of this function exceeds a specified upper limit.

REACHABLE($\boldsymbol{X}_A$, $\boldsymbol{X}_B$)

1 GENERATE_TRAJ($\boldsymbol{X}_A$, $\boldsymbol{X}_B$);
2 for i=1 to N do
3 Flag$_i$ and $J_i \longleftarrow$ INVERSE_PROBLEM(i);
6 if (($\exists$Flag$_i$; $i = 1 \sim N$) =REACHABLE) then
7 CM $\longleftarrow$ OPTIMAL_CM($J_1, \cdots, J_N$);
8 Return TRUE;
9 else Return FALSE;

Fig. 5. Algorithm of REACHABLE

B. Local planning level

In the local planning level, the inverse problem is solved at each instant on a switching time interval, ΔT, for a given object trajectory connecting between a specified two object configuration, $\boldsymbol{X}_A(\boldsymbol{R}_A, \boldsymbol{p}_A)$ and $\boldsymbol{X}_B(\boldsymbol{R}_B, \boldsymbol{p}_B) \in SE(3)$. Next, it checks whether feasible trajectories exist for the multi-fingered hand which would satisfy all manipulation constraints. ΔT can be fixed or selected randomly.

The REACHABLE($\boldsymbol{X}_A$, $\boldsymbol{X}_B$) function in Fig.5 shows the algorithm of a local planner. First, the GENERATE_TRAJ($\boldsymbol{X}_A$, $\boldsymbol{X}_B$) function generates the object trajectory which connects $\boldsymbol{X}_A$ with $\boldsymbol{X}_B$. Trajectories for position, $\boldsymbol{x}(t) \in \Re^3$, and orientation, $\boldsymbol{R}(t) \in SO(3)$ are given by

$$\boldsymbol{x}(t) = d(t)(\boldsymbol{p}_B - \boldsymbol{p}_A) + \boldsymbol{p}_A \quad (13)$$
$$\boldsymbol{R}(t) = \boldsymbol{R}_A \exp(d(t)\phi_E\widehat{\boldsymbol{K}}) \quad (14)$$

where

$$d(t) = -2(t/\Delta T)^3 + 3(t/\Delta T)^2, \quad 0 \leq t \leq \Delta T \quad (15)$$
$$\widehat{\boldsymbol{K}} = \frac{1}{2\sin\phi_E}(\boldsymbol{R}_A^T\boldsymbol{R}_B) \in se(3) \quad (16)$$

Equations (13) $\sim$ (16) satisfy the following boundary conditions

$$\boldsymbol{x}(0) = \boldsymbol{p}_A, \quad \boldsymbol{x}(\Delta T) = \boldsymbol{p}_B, \quad \dot{\boldsymbol{x}}(0) = \dot{\boldsymbol{x}}(\Delta T) = 0 \quad (17)$$
$$\boldsymbol{R}(0) = \boldsymbol{R}_A, \quad \boldsymbol{R}(\Delta T) = \boldsymbol{R}_B, \quad \dot{\boldsymbol{R}}(0) = \dot{\boldsymbol{R}}(\Delta T) = \boldsymbol{0} \quad (18)$$

After generating object trajectories, the INVERSE_PROBLEM function starts to solve the inverse kinematic and dynamic problems at every instant on ΔT for all combinations of contact modes which satisfies (8) and (9) as:

$$6 \leq 3n_R + n_S \leq n_\theta, \quad n_R + n_S = n_C \quad (19)$$

in order that we could obtain solutions for a manipulation system which is kinematically determinate and manipulable. We denote by N shown in Fig.5 the number of all feasible combinations of contact modes which satisfies (19). The kinematics and dynamics of the manipulation system vary according the change of the contact mode. Therefore, changing contact modes makes the forbidden region vary and assist the expansion of the random trees

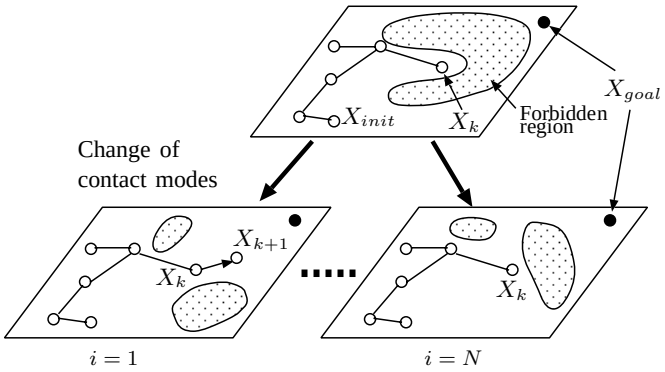

Fig. 6. Change of forbidden regions by switching contact modes

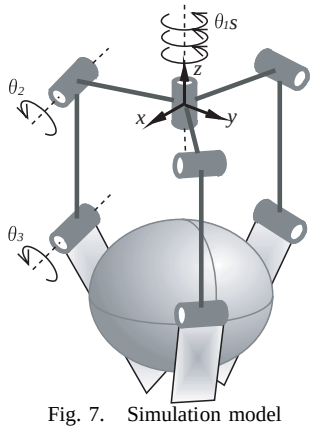

Fig. 7. Simulation model

from the stuck subgoal, (e.g. $\boldsymbol{X}_k$), as shown at the top of Fig.6.

In addition, we calculate a cost functional of the form:

$$J_i(\boldsymbol{X}_A,\ \boldsymbol{X}_B) = \int_0^{\Delta T} L(\boldsymbol{X}(t), \dot{\boldsymbol{X}}(t),\ \boldsymbol{\tau}(t))dt \quad (20)$$

where $\boldsymbol{\tau}$ is joint driving torques. If the inverse problems are solvable for multiple combinations of contact modes through the switching time interval, ΔT, the OPTIMAL_CM function selects the combination of contact mode that minimizes (20). Finally, the REACHABLE function returns TRUE if the trajectories which can connect $\boldsymbol{X}_A$ and $\boldsymbol{X}_B$ are found. Otherwise, it returns FALSE.

IV. COMPUTER SIMULATION

In this section, we verify the effectiveness of the proposed manipulation planning by considering the manipulation system, which consists of one elliptic object and a three 3-degrees of freedom fingered hand with a flat rectangular effector on the third link, as shown in Fig.7. Each first joint of the three fingers locates in the same position, and is independently actuated of the other. Each flat link has the contacts with the object. The radius of the object is 0.2, 0.2 and 0.16 m. The mass of the object is 1.0 kg. The first and second links are 0.14 and 0.2 m long respectively. The dimensions of the third link is 0.2 m by 0.07 m. The mass of each link is 0.5 kg. The coefficient of friction is 0.5.

In order for the manipulation system shown in Fig.7 to be kinematically manipulable and determinate, the following constraints on the number of rolling and sliding contacts are imposed by (19):

$$6 \leq 3n_R + n_S \leq 9 \quad (21)$$

The combinations of contact modes which satisfy (21) results in (i) $n_R = 3,\ n_S = 0$ and (ii) $n_R = 2,\ n_S = 1$. Considering there are three contact points, the number of feasible combinations of contact modes amounts to four combinations, as shown in Table I.

TABLE I
COMBINATIONS OF CONTACT MODES

No.	Finger 1	Finger 2	Finger 3
1	R	R	R
2	R	R	S
3	R	S	R
4	S	R	R

We consider a manipulation task with rotation (the equivalent axis, $\widehat{\boldsymbol{k}}=[-0.5\ 0.5\ \sqrt{0.5}]^T$, and the equivalent angle, $\phi = 30$ deg) and translation($0.02,\ 0.02,\ 0.02$ m in $x,\ y$ and z axis directions) from the initial object configuration. The fixed switching time interval ΔT=1.0 sec. is used. The algorithm was implemented in MATLAB on 1.4 GHz Intel Pentium IV PC with 256 MB of memory running Windows 2000.

We ran the planner four times with different random seeds. The results are shown in Table II. Rows 2-6 list the running time, the number of subgoal candidates generated at random, the number of subgoals that are locally reachable, the ratio of the number of locally reachable subgoals to the number of randomly generated subgoal candidates, and the number of switching, respectively. It takes more than two hours to find feasible solutions since we should solve the problems which involve the complicated dynamics and kinematics of the manipulation system. The probability that randomly assigned subgoal candidates become new subgoals is comperatively high because we take into consideration all combinations of contact modes when we find each new subgoal.

Fig.8 shows the explored subgoals of the object position with respect to the base frame, for the case of example B in Table II. The numbers attached to each subgoal indicate the sequence of the generated subgoals and the contact mode numbers for each of three contact points. Similarly, Fig.9 shows the explored subgoals of the object orientation. The orientation is expressed by a Gauss map for the unit vectors of the principal axes of frame, $\{O\}$, of each subgoal. The initial orientation agrees with the $x,\ y$ and z

TABLE II

PERFORMANCE OF THE PLANNER

Example	A	B	C	D	Ave.
Running time (min.)	201	250	81	85	154
$\boldsymbol{X}_{rand}$	208	303	113	90	179
$\boldsymbol{X}_{i}$	33	31	18	16	25
$\boldsymbol{X}_{rand}/\boldsymbol{X}_{i}$	6.3	9.8	6.3	5.6	7.3
Switching	3	4	2	3	3

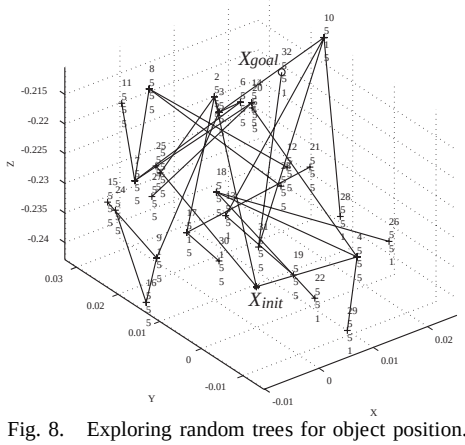

Fig. 8. Exploring random trees for object position.

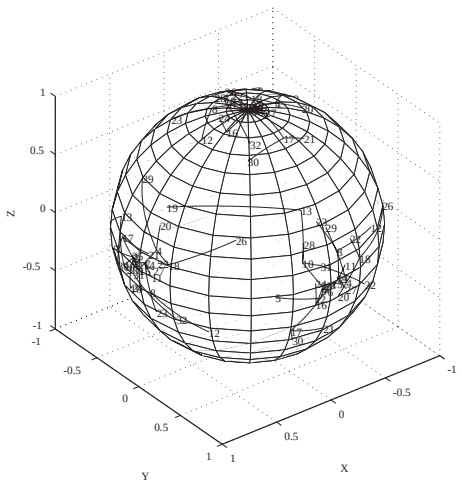

Fig. 9. Exploring random trees for object orientation.

axes in Fig.9. After a total of 303 subgoal candidates were selected at random, 31 subgoals were locally reachable among them. Finally, the trees are extended to the final goal by four times-switching with the transitions of contact modes such as $RRR \rightarrow RRR \rightarrow RSR \rightarrow RRR \rightarrow RRS$, where RSR denotes that each of contact points has rolling, sliding and rolling contact modes. Fig.10 shows snapshots at each switching.

V. CONCLUSION

We proposed new algorithm for manipulation planning with switching contact modes based on the concepts of random trees. Switching contact modes can improve reachability for manipulation planning. These ideas contribute to dextrous manipulation. We showed the validity of the planner by simulating manipulation planning for 3-D manipulation.

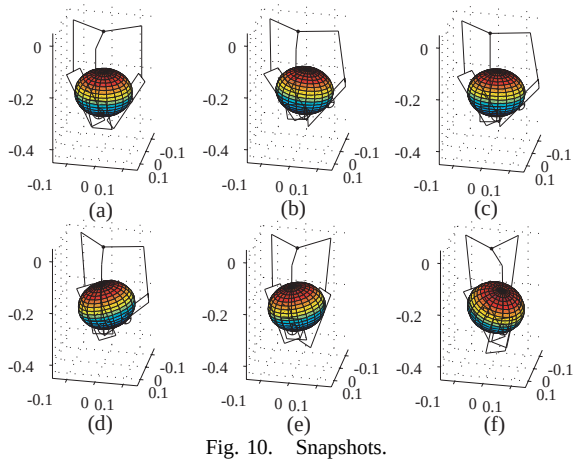

Fig. 10. Snapshots.

VI. REFERENCES

[1] M.J. Cherif, K.K. Gupta, "Planning quasi-static fingertip manipulations for reconfiguring objects", *IEEE Transactions on Robotics and Automation*, vol. 15, no. 11, 1999, pp. 837-848.

[2] A.A. Cole, J.E. Hauser and S.S. Sastry, "Kinematics and control of multifingered hands with rolling contact", *IEEE Transactions on Aotomatical Control*, vol. 34, no. 4, 1989, pp. 398-404.

[3] A.A. Cole, P. Hsu and S.S. Sastry, "Dynamic control of sliding by robot hands for regrasping", *IEEE Transactions on Robotics and Automation*, vol. 8, no. 1, 1992, pp. 42-52.

[4] J.J. Craig, *Introduction to Robotics: Mechanics and Control*, Addison–Wesley Publishing Company, 1989.

[5] R. Kindel, D. Hsu, J.C. Latombe, S. Rock, "Kinodynamic motion planning amidst moving obstacles," in *Proc. of 2000 IEEE Int. Conf. on Robotics and Automation*.

[6] S.M. LaValle, J.J. Kuffner,Jr, "Randomized kinodynamic planning", *The International Journal of Robotics and Research*, vol. 15, no. 5, 2002, pp. 378-400.

[7] D.J.Montana, "The kinematics of contact anf grasp", *Int. Journal of Robotics Research*, vol. 7, no. 3, 1988, pp. 17-32.

[8] R.M. Murray, Z. Li and S.S. Sastry, *A Mathematical Introduction to Robotic Manipulation*, CRC Press, 1993.

[9] N. Sarker, X. Yun and V. Kumar, "Dynamic control of 3-D rolling contacts in two-Arm manipulation", *IEEE Transactions on Robotics and Automation*, vol. 13, no. 3, 1997, pp. 364–376.

[10] J.C. Trinkle, J.J. Hunter, "A framework for planning dextrous manipulation," in *Proc. of 1991 IEEE Int. Conf. on Robotics and Automation*.

[11] M. Yashima and H. Yamaguchi, "Dynamic motion planning whole arm grasp systems based on switching contact modes," in *Proc. of 2002 IEEE Int. Conf. on Robotics and Automation*.

[12] X. Zheng, N. Nakashima and T. Yoshikawa, "On dynamic control of finger sliding and object motion in manipulation with multifingered hands", *IEEE Transactions on Robotics and Automation*, vol. 16, no. 5, 2000, pp. 469–481.